The Journal of Experimental Biology 212, 329-340
Published by The Company of Biologists 2009
doi:10.1242/jeb.024646

Research article

Signaling to the apical membrane and to the paracellular pathway: changes in the cytosolic proteome of *Aedes* Malpighian tubules

Klaus W. Beyenbach[1,*], Sabine Baumgart[2], Kenneth Lau[1], Peter M. Piermarini[1] and Sheng Zhang[2]

[1]Department of Biomedical Sciences, VRT 8004, Cornell University, Ithaca, NY 14853, USA and [2]Proteomics and Mass Spectrometry Core Facility, 143 Biotechnology Building, Cornell University, Ithaca, NY 14853, USA

*Author for correspondence (e-mail: kwb1@cornell.edu)

Accepted 6 November 2008

Summary

Using a proteomics approach, we examined the post-translational changes in cytosolic proteins when isolated Malpighian tubules of *Aedes aegypti* were stimulated for 1 min with the diuretic peptide aedeskinin-III (AK-III, 10^{-7} mol l^{-1}). The cytosols of control (C) and aedeskinin-treated (T) tubules were extracted from several thousand Malpighian tubules, subjected to 2-D electrophoresis and stained for total proteins and phosphoproteins. The comparison of C and T gels was performed by gel image analysis for the change of normalized spot volumes. Spots with volumes equal to or exceeding C/T ratios of ±1.5 were robotically picked for in-gel digestion with trypsin and submitted for protein identification by nanoLC/MS/MS analysis. Identified proteins covered a wide range of biological activity. As kinin peptides are known to rapidly stimulate transepithelial secretion of electrolytes and water by Malpighian tubules, we focused on those proteins that might mediate the increase in transepithelial secretion. We found that AK-III reduces the cytosolic presence of subunits A and B of the V-type H^+ ATPase, endoplasmin, calreticulin, annexin, type II regulatory subunit of protein kinase A (PKA) and rab GDP dissociation inhibitor and increases the cytosolic presence of adducin, actin, Ca^{2+}-binding protein regucalcin/SMP30 and actin-depolymerizing factor. Supporting the putative role of PKA in the AK-III-induced activation of the V-type H^+ ATPase is the effect of H89, an inhibitor of PKA, on fluid secretion. H89 reverses the stimulatory effect of AK-III on transepithelial fluid secretion in isolated Malpighian tubules. However, AK-III does not raise intracellular levels of cAMP, the usual activator of PKA, suggesting a cAMP-independent activation of PKA that removes subunits A and B from the cytoplasm in the assembly and activation of the V-type H^+ ATPase. Alternatively, protein kinase C could also mediate the activation of the proton pump. Ca^{2+} remains the primary intracellular messenger of the aedeskinins that signals the remodeling of the paracellular complex apparently through protein kinase C, thereby increasing transepithelial anion secretion. The effects of AK-III on active transcellular and passive paracellular transport are additive, if not synergistic, to bring about the rapid diuresis.

Key words: cAMP, PKA, Ca^{2+}, PKC, V-type H^+ ATPase, endoplasmin, actin, annexin, adducin.

Introduction

The invertebrate family of kinin peptides is widely distributed in insects, often with several isoforms in a single species (Torfs et al., 1999). The cockroach *Leucophaea* has eight leucokinins, the yellow fever mosquito *Aedes* has three aedeskinins and *Drosophila* has only one drosokinin (Holman et al., 1987; Terhzaz et al., 1999; Veenstra et al., 1997). All three kinins in *Aedes* have diuretic activity in Malpighian tubules *in vitro* (S. A. Schepel, A. J. Fox, F. Tiburcy, A. W. Blum, K.L., T. Sou, R. Nachman and K.W.B., unpublished observations). In particular, aedeskinin-III stimulates the transepithelial secretion of both NaCl and KCl, and it hyperpolarizes the basolateral membrane voltage while reducing the input resistance of principal cells (S. A. Schepel, A. J. Fox, F. Tiburcy, A. W. Blum, K.L., T. Sou, R. Nachman and K.W.B., unpublished observations). These effects duplicate those of leucokinin-VIII in *Aedes* Malpighian tubules (Beyenbach, 2003; Pannabecker et al., 1993). As shown in Fig. 1, leucokinin-VIII brings about the non-selective stimulation of both NaCl and KCl secretion by increasing the transepithelial secretion of Cl^- (Yu and Beyenbach, 2001; Yu and Beyenbach, 2002; Yu and Beyenbach, 2004). Specifically, the kinins increase the paracellular Cl^- conductance to such an extent as to produce nearly a transepithelial short-circuit, as indicated by the sudden drop of the transepithelial voltage from 59 mV to 5 mV (Fig. 1C). In parallel, the transepithelial resistance plummets from 18.4 kΩcm to 3.2 kΩcm, reflecting the increase in paracellular Cl^- conductance, and the apical and basolateral membrane voltages converge to values only 5 mV apart (Fig. 1B,C).

The increase in paracellular Cl^- conductance affects secondarily an increase in the transcellular secretion of Na^+ and K^+ transport because the transcellular transport pathway for cations is electrically coupled to the paracellular transport (Beyenbach, 2001; Beyenbach, 2003). Thus, for every cation secreted via the transcellular pathway, a Cl^- ion is secreted through the paracellular pathway, bringing about equimolar secretion rates of cations and anions (Fig. 1D).

The on/off effects of kinins on the paracellular Cl^- conductance proceed with switch-like speed (Fig. 1C), suggesting post-translational modifications of the paracellular pathway. Changes in intracellular [Ca^{2+}] appear to mediate the switch-like changes of the paracellular Cl^- conductance. How Ca^{2+} effects sudden changes in paracellular Cl^- conductance has piqued our curiosity. Using the methods of proteomics, we looked for cytosolic proteins associated with Ca^{2+} signaling to the paracellular pathway. We compared the

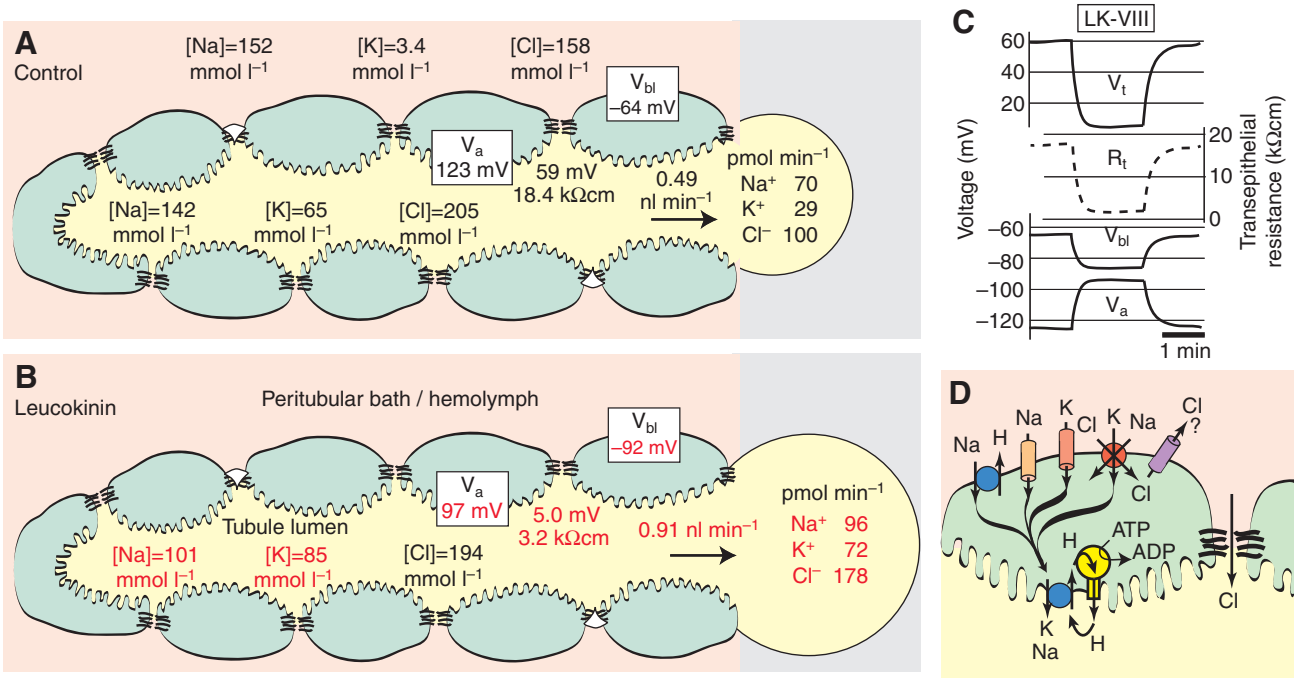

Fig. 1. Leucokinin increases the paracellular Cl^- conductance in Malpighian tubules of *Aedes aegypti*. (A,B) Leucokinin-VIII increases the transepithelial secretion of both NaCl and KCl. Numbers in red indicate a statistical significant difference (P<0.05) from controls; (C) electrophysiological effects of LK-VIII on the transepithelial voltage (V_t) and resistance (R_t) and on the basolateral and apical membrane voltages (V_{bl}, V_a) indicate a transepithelial short-circuit brought about by the sudden increase in paracellular Cl^- conductance; (D) model of transepithelial electrolyte secretion in *Aedes* Malpighian tubules. The transepithelial transport of Na^+ and K^+ is active and mediated by principal cells; the transepithelial transport of Cl^- is passive and mediated by the paracellular pathway and stellate cells. However, under conditions of diuresis triggered by aedeskinin or kinin isoforms, the transcellular and paracellular pathways are electrically so well coupled that the rates of transcellular cation secretion and paracellular anion secretion are equivalent (Beyenbach, 2003; Hayes et al., 1989; Pannabecker et al., 1993; Yu and Beyenbach, 2004).

cytosolic proteome and phosphoproteome of Malpighian tubules before and after stimulation with 10^{-7} mol l^{-1} aedeskinin-III for only 1 min. From the many proteins that were down- or up-regulated in the cytosol, we present here those that might be associated with stimulating transepithelial transport. We found evidence for aedeskinin-III signaling to the cytoskeleton, where Ca^{2+} and protein kinase C appear to trigger the remodeling of septate junctions with likely consequences for the integral membrane proteins that define the paracellular Cl^- permselectivity and conductance. In addition, we found evidence for signaling to the transcellular pathway, where protein kinase A (PKA) might induce the assembly and activation of the V-type H^+-ATPase at the apical membrane through a cAMP-independent mechanism. Alternatively, protein kinase C could bring about the assembly and activation of the V-type H^+-ATPase. Thus, insect kinins appear to activate both paracellular and transcellular transport pathways. The additive or perhaps synergistic effects of stimulating both transport pathways are consistent with the rapid increase in the transepithelial secretion of NaCl and KCl that we and others have previously reported (Coast, 1995; Hayes et al., 1989; O'Donnell and Spring, 2000; Pannabecker et al., 1993).

Materials and methods

Mosquitoes and Malpighian tubules

The mosquitoes (*Aedes aegypti* L.) were reared and maintained in the laboratory at 28°C as described by Pannabecker and colleagues, with the exception that we fed larval mosquitoes Tetramin flakes (tropical fish food) ground to a powder with a mortar and pestle (Pannabecker et al., 1993). Malpighian tubules were dissected exclusively from adult female mosquitoes (3–7 days old). After cold-anesthetizing a mosquito on ice, the mosquito was decapitated and submerged in Ringer solution. By holding the thorax with one pair of forceps (Dumont #5, Fine Science Tools, Foster City, CA, USA) and gently pulling at the rectum with another pair of forceps, the intestine and Malpighian tubules were freed from the abdomen. The five Malpighian tubules were removed from their attachment to the intestine and transferred to a 1.5 ml low-adhesion microcentrifuge tube (USA Scientific, Ocala, FL, USA) containing 0.5 ml Ringer solution at room temperature. The Ringer solution contained the following, in mmol l^{-1}: 150 NaCl, 3.4 KCl, 25 HEPES, 1.8 $NaHCO_3$, 1.0 $MgSO_4$, 1.7 $CaCl_2$ and 5.0 glucose. The pH was adjusted to 7.1 using 1 mol l^{-1} NaOH.

To isolate enough cytosolic protein for proteomic analyses, it was necessary to collect more than 2000 Malpighian tubules each for both a control group (C) and an aedeskinin-treated (T) group. On a typical tubule collection day, several volunteers in the lab collected about 250 tubules each for C and T groups. The tubules of each group were pooled into separate microcentrifuge tubes containing 200 µl of Ringer. In the case of C tubules, the Ringer solution was withdrawn after the tubules had settled to the bottom of the vial. The tubules were subsequently frozen in liquid nitrogen. In the case of T tubules, they were resuspended in 200 µl of Ringer containing 10^{-7} mol l^{-1} aedeskinin-III. After treating the tubules for only 1 min with aedeskinin-III, the Ringer was removed and the tubules were frozen in liquid nitrogen. C and T tubules were stored at –80°C until the extraction of cytosolic proteins. The isolation sessions were repeated until we had collected 2378 tubules for the control group and 2468 tubules for aedeskinin-treated group.

Extraction of cytosolic proteins

On the day of the extraction, C and T tubules were thawed on ice. Ice-cold extraction buffer (100 µl) was added to each. The extraction buffer contained, in mmol l^{-1}: 50 HEPES (pH 7.1), 10 dithiothreitol, 1 PMSF (phenylmethylsulfonyl fluoride) and 5 EDTA (ethylenediaminetetraacetic acid). The extraction buffer was supplemented with 1% Halt Protease Inhibitor Cocktail and 2% Phosphatase Inhibitor Cocktail (Pierce Biotechnology, Rockford, IL, USA) and 0.10% Triton X-100. The tubules were then homogenized using a plastic pestle. In addition, the tubules were rapidly passed back and forth through a 200 µl pipette tip in order to mechanically dissociate and lyse cells. As multiple microcentrifuge tubes of C and T tubules were collected, the homogenates were pooled for each group. The pooled homogenates were brought up to 1 ml volume with extraction buffer. As a final disruption and lysis step, the pooled homogenates were sonicated with a Model 250 Ultrasonic Cleaner (RAI Research, Hauppauge, NY, USA) for 30 s.

To precipitate cell debris, the pooled homogenates were centrifuged at 3000 ***g*** at 4°C for 10 min. The supernatant was subsequently removed and centrifuged further at 100,000 ***g*** and 4°C for 60 min using an OptimaMax ultracentrifuge (Beckman). The high-speed centrifugation separated the cytosolic-protein fraction (supernatant) from the membrane-protein fraction (pellet). The cytosolic fraction (~900 µl) was transferred to a low-adhesion microcentrifuge tube (USA Scientific) and kept on ice, whereas the membrane fraction was washed three times with extraction buffer and then stored at –80°C. To estimate the concentration of protein in the cytosolic fraction, a Bradford protein assay (BioRad, Hercules, CA, USA) was performed on a 20 µl aliquot using bovine serum albumin as a reference standard. The protein concentration in the extract prepared from C tubules was 0.68 µg $µl^{-1}$ and 0.84 µg $µl^{-1}$ in that prepared from T tubules. Total protein amounted to 789 µg in the case of C tubules and 966 µg for T tubules. The cytosolic extracts were submitted for proteomic analysis to the Cornell University Life Sciences Proteomics and Mass Spectrometry Core Facility (Ithaca, NY, USA).

Proteomic analysis

The technical details of the proteomic analysis are described by Yang and colleagues (Yang et al., 2007). For the reader of *The Journal of Experimental Biology*, we focus here on the major proteomic steps and on the experimental design and data analysis.

Our study aimed to identify the cytosolic proteins that change after stimulating Malpighian tubules with aedeskinin-III using the methods of 2-D gel electrophoresis and mass spectrometry (Fig. 2). Approximately 180 µg of cytosolic protein from the control (C) and aedeskinin-III-treated (T) tubules were used for the 2-D gel analyses. The first-dimensional separation was performed by immobilized pH gradient isoelectric focusing (24 cm IPG, nonlinear pH 3–10 strips; GE Healthcare, Piscataway, NJ, USA). For electrophoresis in the second dimension, 12.5% homogenous SDS–polyacrylamide DALT gels were cast using the DALT*six* gel casting system (GE Healthcare). Peppermint-Stick molecular mass markers were applied to each gel at a concentration of 0.25 µg/protein.

Gels were subsequently incubated with Pro-Q Diamond stain for the selective detection of phosphoproteins. Importantly, the Pro-Q Diamond stain suggests, but does not prove, the presence of phosphorylation. Immediately after gel image scanning, the SYPRO Ruby stain was used for total protein staining in the same gel (Fig. 2).

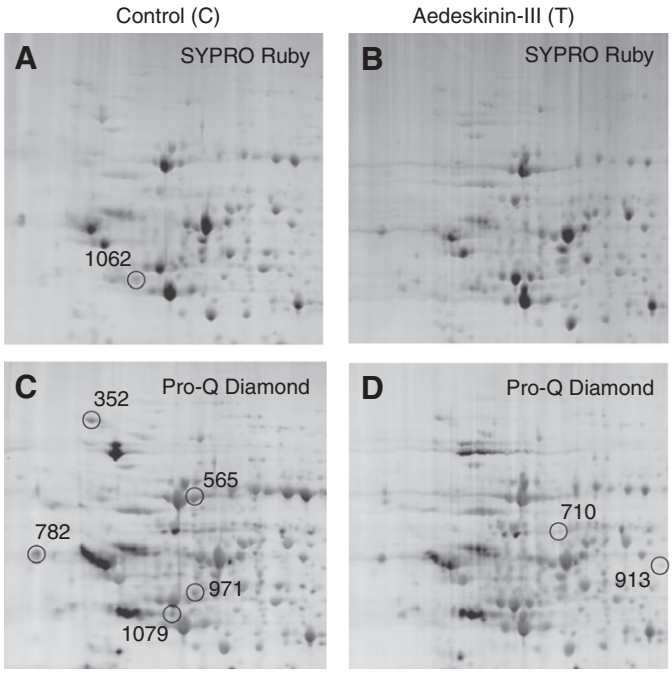

Fig. 2. Two-dimensional electrophoresis of cytosolic proteins before (control, C) and after treating (T) Malpighian tubules with aedeskinin-III (10^{-7} mol l^{-1}) for 1 min. Portions of the whole gel are shown. The SYPRO Ruby stain recognizes proteins, and the Pro-Q Diamond stain recognizes phosphoproteins. Circles identify some of the spots of interest in the present study: 352, endoplasmin; 565, subunit A of the V-type H^+ ATPase; 710, subunit B of the V-type H^+ ATPase; 782, subunit B of the V-type H^+ ATPase and calreticulin; 913, adducin; 971, rab dissociation inhibitor; 1062, regulatory subunit type II of protein kinase A; 1079, actin (see also Table 1).

The 2-D gels were run in duplicate, yielding two SYPRO Ruby and two ProQ Diamond gel images for each control and treated samples. Approximately 1500 spots were detected in each gel, where up to five different proteins were identified in some spots. Spots selected for protein identification had to be present in all four gels, except for 'unmatched' spots that were present in both C gels but not in both T gels or *vice versa*.

The image (spot) analysis software (Image Master 2D Platinum, 6.0; GE Healthcare) produces 3-D images of spot volumes and determines the volume of each spot in the gel (Fig. 3). As duplicate gels yield two C spot volumes and two T spot volumes, a significant difference between C and T spot volumes is evaluated by the C/T ratio, using values that minimize the difference between T and C spot volumes. The following example illustrates the calculation. Suppose that the two C spot volumes are 33 and 35 (arbitrary units), and the two T spot volumes are 25 and 27. The minimum difference between C and T is between 33 and 27. The C/T ratio is therefore 33/27=1.22. A negative sign is assigned to that value (–1.22) to indicate a decrease in spot volume in the T gel. Thus, our criterion of C/T≥±1.5 selects obvious spot volume changes. A criterion of C/T≥±2.0 would have been too stringent and excluded all changes in spot volume.

Spots of interest were robotically picked (Investigator ProPic; Genomic Solutions, Ann Arbor, MI, USA) for in-gel digestion with trypsin and extraction by robotic ProPrep (Genomic Solutions, Ann Arbor, MI, USA) using the standard protocol described by Shevchenko and colleagues (Shevchenko et al., 1996). Gel-

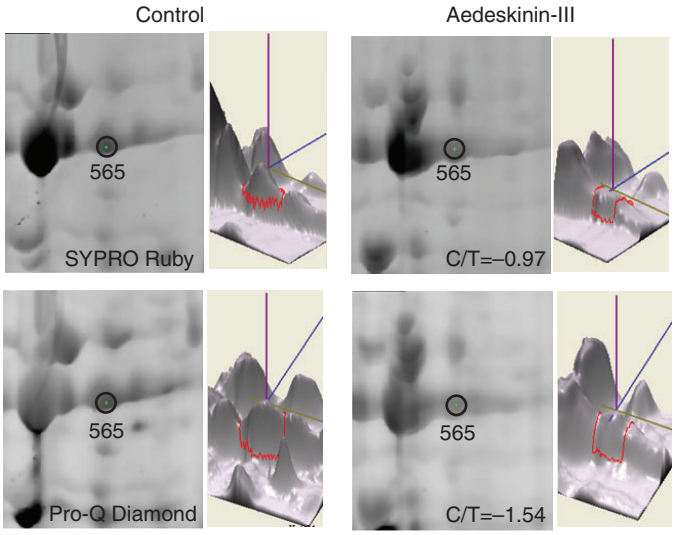

Fig. 3. Effect of aedeskinin-III (10^{-7} mol l^{-1}) on subunit A (spot 565) of the V-type H^+ ATPase in the cytosol of *Aedes* Malpighian tubules. Negative SYPRO Ruby and Pro-Q Diamond C/T ratios indicate reductions in protein concentration and phosphorylation. Spot 565 was selected for analysis because the phosphorylation C/T ratio exceeded the criterion of ±1.5.

extracted peptides were loaded onto a C18 PepMap trap column and eluted in a 30-min gradient of 5% to 45% acetonitrile in 0.1% formic acid. The eluted peptides were fed into an in-line hybrid triple-quadrupole linear ion trap mass spectrometer (4000 Q Trap from ABI/MDS Sciex, Framingham, MA, USA, equipped with a Micro Ion Spray Head II ion source).

The mass spectrometry (MS) data were acquired using the Analyst 1.4.2 software (Applied Biosystems, Foster City, CA, USA) in the positive ion mode for information-dependent acquisition (IDA) analysis. The IDA analysis surveyed each scan between *m*/*z* 375 and *m*/*z* 1550, where *m*/*z* is the mass-to-charge ratio. A subsequent enhanced resolution scan selected the three highest intensity ions (peptides) with multiple charge states for tandem MS (MS/MS).

The MS/MS data generated from the IDA analysis were submitted to Mascot 2.2 for database search using an in-house licensed Mascot local server and the combined *Aedes aegypti* and *Anopheles gambiae* databases downloaded from NCBInr (November 2007), allowing for one missed cleavage site by trypsin. The peptide tolerance was set to 1.2 Da and MS/MS tolerance was set to 0.6 Da. The following were set as variables: carbamidomethyl modification of cysteine, methionine oxidation and phosphorylation of serine/threonine and tyrosine. Protein identifications were considered for peptides only if their score defined by Mascot probability analysis was greater than their 'identity' score (www.matrixscience.com/help/scoring_help.html#PBM). For multiple proteins identified in single spots, an exponential modified protein abundance index (emPAI) was used to correctly distribute the change in expression determined by the in-gel staining and image analysis to each of the proteins comprising a spot (Yang et al., 2007).

Ramsay fluid secretion assays

The rate of transepithelial fluid secretion was measured in isolated Malpighian tubules by a modified method of Ramsay (Ramsay, 1953). After isolating a Malpighian tubule from a female mosquito, the tubule was transferred to a Ringer droplet of 50 µl under light mineral oil. The proximal end of the tubule was pulled into the oil with the aid of a glass hook, leaving the distal blind end in the Ringer droplet. Half-way between the glass hook and the oil–water interface, a stellate cell was nicked with a fine needle so that fluid secreted by the epithelial cells could exit the lumen into the oil. Timed volumes of secreted fluid were measured with an ocular micrometer, taking into consideration the volume occupied by the tubule segment within the secreted droplet. After measuring control secretion rates for 30 min, aedeskinin-III was added to the peritubular medium to yield a concentration of 10^{-6} mol l^{-1}. After another 30 min, H89 was added to the peritubular Ringer solution, to test the effect of this PKA inhibitor on transepithelial fluid secretion.

All aedeskinins were synthesized in the laboratory of Nachman (Zubrzak et al., 2007). The calcitonin-like diuretic peptide AnogaDH31 was a gift of David Schooley (University of Nevada). The inhibitor of protein kinase A – H-89 – was purchased from Sigma (St Louis, MO, USA). It is well known that inhibitors are not ideally selective, and inhibitors of kinases are no exception (Davies et al., 2000). In the present study, we used H-89 at a concentration that is 2.5 times lower than the concentration used to establish the role of PKA in the activation of the V-type H^+ ATPase in the blowfly salivary gland (Voss et al., 2007).

cAMP assay

Cytosolic cAMP concentrations were measured in sets of 20 Malpighian tubules isolated from adult female mosquitoes 3–7 days old. One set of tubules served as the control group (C) and the other as the aedeskinin-treated (T) group. The tubules were pooled together in 1.5 ml low-adhesion microcentrifuge tubes (USA Scientific) containing 0.1 ml Ringer solution supplemented with 0.5 mmol l^{-1} isobutylmethylxanthine (IBMX, Sigma), an inhibitor of phosphodiesterase. After 15 min incubation at room temperature, sets of tubules were treated with Ringer solution (negative control), aedeskinin-I, –II or –III (10^{-6} mol l^{-1}) or Anoga DH_{31} (10^{-6} mol l^{-1}) for 2 min at room temperature. Anoga DH_{31} is a calcitonin-like peptide that is known to increase the intracellular concentrations of cAMP in *Aedes* Malpighian tubules (Coast et al., 2005). Thereafter, the Ringer solution was removed and the tubules were frozen in liquid nitrogen. The tubules were then stored at –80°C.

For the extraction of cAMP, the tubules were thawed on ice and homogenized in their microcentrifuge tube with a plastic pestle in 100 µl of ice-cold 100% ethanol containing 0.5 mmol l^{-1} IBMX. After rinsing the pestle with 100 µl of ice-cold 100% ethanol containing 0.5 mmol l^{-1} IBMX, the tubules were further homogenized by (1) passing them back and forth through a 200 µl pipette and vortexing them for 1 min and then (2) sonicating them for 1.5 min.

The homogenates were centrifuged at 3000 ***g*** at 4°C for 10 min. The supernatant was transferred to a new microcentrifuge tube, whereas the remaining pellet (containing precipitated protein) was used to determine the protein concentration by using a BCA protein assay (Thermo Fisher Scientific, Rockford, IL, USA). The microcentrifuge tube containing the supernatant was placed in a water bath at 100°C for ~11 min in order to evaporate the ethanol and to bring the isolated cAMP to dryness. The resulting residue was subsequently resuspended in 200 µl of cAMP Assay Buffer (provided in the CatchPoin cAMP Assay Kit, Molecular Devices, Sunnyvale, CA, USA) containing 0.5 mmol l^{-1} IBMX.

Cyclic-AMP concentrations were measured with a competitive immunoassay, the CatchPoint cyclic-AMP Fluorescent Assay Kit

(Molecular Devices, Sunnyvale, CA, USA). In brief, samples and cAMP standards were placed in a 96-well plate coated with goat anti-rabbit IgG. Rabbit anti-cAMP antibody and horseradish-peroxidase-labeled cAMP conjugate were added to each well and left to incubate at room temperature for 2 h. The wells were then washed six times with 200 µl 1×Wash Buffer (containing 0.02 mol l^{-1} Tris, 150 mmol l^{-1} NaCl, 0.05% Tween 20 and 0.05% Proclin 200, pH 7.4). After a 10-min incubation with a fluorogenic substrate of horseradish peroxidase (Stoplight Red), the plate was read at 540 nm using the Biotek Synergy 2 Multi-Detection Microplate Reader (BioTek Instruments, Winooski, VT, USA). A standard curve of cAMP concentrations was generated with the GraphPad Prism software (GraphPad Software, La Jolla, CA, USA), and cAMP concentrations of unknown samples were determined from this standard curve.

Electron microscopy

Malpighian tubules were prepared for electron microscopy as described previously (O'Connor and Beyenbach, 2001). Sections were cut to a thickness of 70 nm and stained with osmium tetroxide. Electron micrographs of the tubules were produced with a Philips Tecnai 12 Biotwin transmission electron microscope (FEI, Eindhoven, Netherlands).

Results

Proteomic experimental design and data analysis

The 2×2 design of the experiment allowed four comparisons between gels (Fig. 2). The comparison of C and T SYPRO Ruby gels reveals changes in protein abundance, whereas the comparison of C and T Pro-Q Diamond gels reveals changes in the levels of phosphoproteins. Vertical comparisons between SYPRO Ruby and Pro-Q Diamond gels help identify spots containing phosphoproteins. The Pro-Q Diamond stain detects phosphate groups linked to tyrosine, serine or threonine residues (phosphorylations), but it also detects the phosphate groups of nucleotides if these are covalently bound to protein (Molecular Probes, Invitrogen, Carlsbad, CA, USA).

The 2-D gel electrophoresis detected a total of 1488 spots in SYPRO Ruby and Pro-Q Diamond stains (Fig. 2). Applying the criterion of a ±1.5-fold change in C/T ratio between C and T gels, the SYPRO Ruby stain detected 26 spots in the C gel that decreased in the T gel. Of these 26 spots, 12 did not appear in the T gel and are therefore considered 'unmatched'. The SYPRO Ruby stain also found 21 spots that increased in intensity in the T gel. Of these 21 spots, five are uniquely present in the T gel and are considered 'unmatched'.

The Pro-Q Diamond stain identified 81 spots in the C gel and 75 spots in the T gel (Fig. 2). Thus, approximately 5% of the spots detected by SYPRO Ruby contain phosphoproteins. The criterion of a ±1.5-fold change in C/T ratio revealed 19 spots in the C gel that decreased in intensity in the T gel. Of these 19 spots, three did not appear in T gel and are considered 'unmatched'. Of the 75 spots staining positively for Pro-Q Diamond in the T gel, seven spots increased in volume over those in the C gel. The loss of phosphoproteins in 19 spots and the increase in phosphoproteins in seven spots suggest that, overall, aedeskinin-III causes more dephosphorylation than phosphorylation.

The protein identification in spots with C/T ratios >±1.5 yielded 128 cytosolic proteins that are affected by the 1 min treatment with aedeskinin-III. From these, we consider here only those proteins that might be associated with aedeskinin signaling and the consequent increase in fluid secretion (Table 1).

Subunit A of the V-type H^+ ATPase

Subunit A of the V-type H^+ ATPase was found in a single spot (#565) in both C and T gels (Table 1; Fig. 3). With a protein score of 639 and 26 unique peptides, it is the best identified protein of them all. Unique peptides are those peptides (amino acid sequences) that collectively are unique for the protein thus identified. Comparing C and T gels reveals that aedeskinin-III decreases the quantity of subunit A in the cytosol of Malpighian tubules (Fig. 3). Comparing SYPRO Ruby and Pro-Q Diamond ratios, –0.97 and –1.54, respectively, indicates that the loss of phosphoprotein is greater than that of protein.

Subunit B of the V-type H^+ ATPase

Subunit B of the V-type H^+ ATPase and calreticulin shared spot 782 in the C gel (Table 1). The values of protein coverage indicate that subunit B is the less-abundant protein, contributing about 21% of the protein present in this spot. The SYPRO Ruby and Pro-Q Diamond ratios, –0.92 and –1.62, respectively, mirror the fate of subunit A. Again, the loss of phosphoprotein from the cytosol is greater than the loss of protein, consistent with the movement of subunits A and B from the cytosol to the plasma membrane (Table 1).

Of interest is the appearance of subunit B in a new location of the T gel, appearing in spot 710 as the third of four proteins present in this spot (Table 1). As spot 710 in the T gel is at a more alkaline location – that is, to the right of spot 782 in the C gel (Fig. 2) – spot 710 might contain unphosphorylated subunit B.

Calreticulin

Calreticulin is the major protein (79%) in spot 782 shared with subunit B in the C gel (Table 1). Calreticulin is a ubiquitous low-affinity and high-capacity Ca^{2+}-binding protein. The negative C/T ratios of SYPRO Ruby and Pro-Q Diamond stains reflect the removal of calreticulin from the cytosol after treating tubules with aedeskinin-III. Although subunit B in spot 782 might be phosphorylated, we cannot rule out that calreticulin is also phosphorylated.

Endoplasmin

Endoplasmin drew our attention in view of a Pro-Q Diamond ratio of –1.67 as a single protein in spot 352 of the C gel (Table 1). The SYPRO Ruby ratio is –1.0, which indicates that aedeskinin-III removes endoplasmin from the cytosol. The Pro-Q Diamond ratio indicates that the loss of phosphoprotein from the cytosol is greater than the loss of protein. Like calreticulin, endoplasmin is a major Ca^{2+}-binding protein. Endoplasmin is also a molecular chaperone of the heat-shock protein 90 class located in the endoplasmic reticulum.

Actin

Like endoplasmin, actin appeared as the single protein in a spot on the C gel, spot 1079. The high Pro-Q Diamond ratio of –1.67 signals the loss of phosphoprotein from the cytosol when tubules are treated with aedeskinin-III (Table 1). The SYPRO Ruby ratio of +1.21 indicates the increase in cytosolic actin after treating tubules with aedeskinin. Thus, aedeskinin-III appears to increase cytosolic actin at the expense of phosphorylated actin.

Annexin

Spot 1437 contains the single protein annexin. The SYPRO Ruby C/T ratio of –1.57 indicates the significant reduction of annexin in the cytosol after treating tubules with aedeskinin-III (Table 1).

Table 1. Effects of aedeskinin-III (10^{-7} mol l^{-1}) on cytosolic proteins of Malpighian tubules of *Aedes aegypti*

Control (C) spot # (proteins/spot)	SYPRO[1] Ruby (ratio)	Pro-Q[1] Diamond (ratio)	*Aedes aegypti* protein	NCBI accession number	% Sequence coverage[2]	Protein score[3]	Protein mass (PI)[4]	Number of unique peptides[5]	emPAI[6]
565 (1)	–0.97	–1.54	Subunit A, V-type H^+ ATPase	O16109	39.9	639	68,528 (5.26)	26	2.08
782 (2)	–0.92	–1.62	Calreticulin	EAT47943	17.7	204	46,983 (4.42)	10	0.72
			Subunit B, V-type H^+ ATPase	AAD27666	5.8	76	55,466 (5.38)	3	0.19
352 (1)	–1.0	–1.67	Endoplasmin	EAT34979	14.6	283	91,129 (4.81)	15	0.53
1079 (1)	1.21	–1.52	Actin	EAT43989	11.7	141	42,058 (5.30)	3	0.26
1437 (1)	–1.57	–	Annexin	ABF18321	28.4	174	35,828 (4.67)	13	1.42
1062 (4)	–2.20	–1.21	Conservative hypothetical protein	EAT41771	26.7	293	49,824 (5.06)	13	1.61
			cAMP-dependent PK type II regulatory subunit	EAT38936	15.4	84	34,956 (5.49)	5	0.44
971 (4)	–1.71	–1.86	Conservative hypothetical protein	EAT45856	40.3	367	48,726 (5.33)	19	2.25
			rab GDP-dissociation inhibitor (GDI)	EAT34894	10.8	96	50,195 (5.38)	4	0.21
Aedeskinin (T) spot # (proteins/spot)	SYPRO Ruby (ratio)	Pro-Q Diamond (ratio)	*Aedes aegypti* protein	NCBI accession number	% Sequence coverage	Protein score	Protein mass (PI)	Unique peptides	emPAI
710 (4)	1.47	1.68	Aldehyde dehydrogenase,	EAT38124	21.1	249	53,037 (5.66)	11	0.94
			α-esterase	EAT32300	17.4	143	56,899 (5.28)	8	0.48
			Subunit B, V-type H^+ ATPase	AAD27666	14.9	141	55,466 (5.38)	7	0.50
913 (2)	1.69	1.62	Adducin	EAT36850	15.7	317	79,998 (6.27)	14	0.56
			F_0F_1-synthase (β subunit)	ABF18266	16.7	204	53,937 (5.03)	7	0.51
1314 (2)	1.22	1.74	Regucalcin/SMP30,	ABF18387	29.3	325	36,981 (5.19)	13	2.62
			Serine protease inhibitor 4 (serpin-4)	EAT40507	9.8	108	42,596 (5.65)	3	0.25
2103 (1)	Unmatched	1.05	Actin-depolymerizing factor	ABF18522	13.5	110	17,323 (6.74)	2	0.43

The list of proteins is a subset of over 100 cytosolic proteins that changed significantly after aedeskinin treatment.

[1]Ratio of spot volumes in control gel (C) and treated gel (T), C/T, after 1 min treatment with 10^{-7} mol l^{-1} aedeskinin-III. Positive and negative ratios indicate, respectively, an increase and decrease in spot volume after treatment with aedeskinin. Absolute values less than 1 indicate that spot volumes overlapped, diminishing their difference. Only spots with absolute ratios ≥1.5 were considered significant. See Materials and methods for further detail.

[2]Percentage sequence coverage tells the percentage of residues determined before a protein was identified (obtained from Mascot search output with peptide ion score cutoff set at 20).

[3]Protein score is the MudPIT score from Mascot search requiring top rank hit and an ion score cutoff set at 20. The higher the protein score the greater the confidence in the protein identification (correlating with percentage sequence coverage).

[4]Isoelectric point.

[5]Number of peptides in the tryptic digest that are known to be present in the protein of interest.

[6]emPAI estimates the mol fraction of proteins in case of multiple proteins per spot. In the case of spot 782, calreticulin contributes 79% to the spot volume and subunit B contributes 21%, calculated as % of total emPAI.

Although annexin is known to be phosphorylated (Rescher et al., 2008), the Pro-Q Diamond stain did not detect phosphoproteins in spot 1437.

cAMP-dependent PK type II regulatory subunit

The regulatory subunit II of the cAMP-dependent protein kinase surfaced in spot 1062 as one of four proteins (Table 1). As the second most-abundant protein in spot 1062, the regulatory subunit II contributes approximately 29% of the protein present in spot 1062. The C/T ratios of –2.20 and –1.21, respectively, for SYPRO Ruby and Pro-Q Diamond stains indicate a marked reduction of protein in the cytosol, far greater than the reduction in phosphoprotein, consistent with protein degradation.

rab GDP-dissociation inhibitor

Spot 971 consists of four proteins, including the rab GDP-dissociation inhibitor (GDI), which contributes approximately 13% of the protein in this spot. The similar C/T ratios, –1.71 and –1.86,

respectively, for SYPRO Ruby and Pro-Q Diamond stains, suggest that the removal of protein from the cytosol is the primary mechanism for removing the phosphate signal.

Adducin

Spot 913 in the T gel is occupied by two proteins: adducin and the β-subunit of the mitochondrial ATPase (Table 1). Adducin accounts for 52% of the protein present in spot 913. The similar C/T ratios, +1.69 and +1.62 for SYPRO Ruby and Pro-Q stains, respectively, indicate (1) a major increase in cytosolic adducin and/or the β subunit of the mitochondrial F_0F_1 synthase, and (2) a major increase in the phosphorylated form of one or both proteins, after treating Malpighian tubules with aedeskinin-III. Thus, aedeskinin-III adds phosphoproteins of adducin and/or β subunit to the cytosol. In view of the 14 and seven unique peptides identified in the case of adducin and the β subunit of the F_0F_1 synthase, respectively, we have higher confidence in the increase of adducin than in the increase in the β subunit of the F_0F_1 synthase.

Regucalcin

Spot 1314 in the T gel reveals two proteins – regucalcin and serpin-4 (Table 1). As regucalcin contributes 91% of the protein in the spot, the significant increase in C/T ratios is likely to include the arrival of new regucalcin in the cytosol after treating Malpighian tubules with aedeskinin-III. The new regucalcin arrives in the cytosol as a phosphoprotein. Regucalcin is a Ca^{2+}-binding protein.

Actin-depolymerizing factor

The SYPRO Ruby stain reveals spot 2103 present in the T gel but not in the C gel. The unmatched presence of this spot in the T gel indicates the arrival of a new protein in the cytosol when Malpighian tubules are stimulated with aedeskinin-III (Table 1). The new arrival is actin-depolymerizing factor (ADF). It is the single protein of spot 2103. The positive Pro-Q Diamond C/T ratio of 1.05 identifies ADF as a phosphoprotein in the cytosol.

As the proteomic data indicated that treating Malpighian tubules with aedeskinin-III for 1 min results in the cytosolic loss of (1) two subunits of the V-type H^+ ATPase and (2) the regulatory subunit of protein kinase A (PKA), we examined the role of PKA in mediating the diuretic effects of aedeskinin by using a PKA inhibitor in the Ramsay fluid secretion assay and measuring intracellular cAMP concentrations after stimulating tubules with aedeskinin-III.

Ramsay fluid secretion assay

Using the modified method of Ramsay, we examined whether the mechanism of action of aedeskinin-III involves PKA. The rate of fluid secretion was 0.19±0.04 nl min^{-1} in 10 Malpighian tubules under control conditions (Fig. 4). The addition of 1 μmol l^{-1} aedeskinin-III to the peritubular bath significantly (P<0.0018) increased the rate of fluid secretion to 0.63±0.13 nl min^{-1} in the same 10 tubules. The subsequent addition of 20 μmol l^{-1} H89 – an inhibitor of PKA – to the peritubular bath significantly reduced the rate of fluid secretion back to control rates.

Intracellular cAMP concentrations

An increase in intracellular cAMP concentration is known to activate PKA. Thus, if aedeskinins stimulate the activity of PKA through 'traditional' means, we would expect to see a rise in intracellular cAMP concentrations after tubules are stimulated with aedeskinin. Sets of 20 Malpighian tubules were exposed to 1 μmol l^{-1} concentrations of aedeskinins-I, -II and -III for 2 min. For a positive control, another set of 20 Malpighian tubules was exposed to an identical concentration of Anoga-DH_{31}, which is known to elevate intracellular concentrations of cAMP in Malpighian tubules (Coast et al., 2005). Under non-stimulated conditions (control), the mean cAMP content of Malpighian tubules was 0.18±0.03 pmol μg^{-1} protein in 12 determinations of 20 tubules each. As shown in Fig. 5, none of the aedeskinins had significant effects on intracellular cAMP concentrations relative to control tubules even though (1) aedeskinin concentrations were 10-fold greater than in the proteomic protocol and (2) tubules were exposed to aedeskinins for 2 min rather than 1 min in the proteomic protocol. By contrast, cytosolic cAMP levels increased more than six fold in the presence of Anoga-DH_{31} compared with controls. Thus, the activation of PKA (suggested by the proteomic data and the effects of H89) is apparently mediated by a 'non-traditional' mechanism that is independent of intracellular cAMP concentrations.

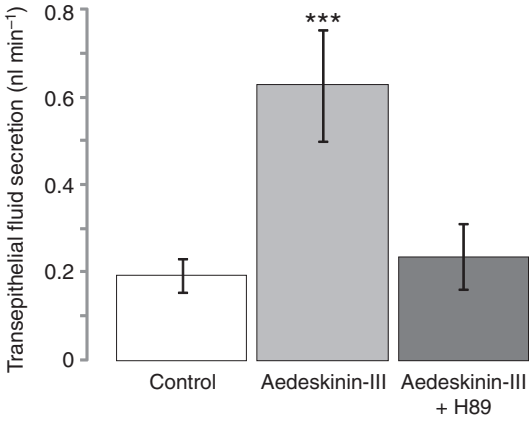

Fig. 4. The PKA inhibitor H89 reverses the diuretic effect of aedeskinin-III in isolated Malpighian tubules of *Aedes aegypti*. Each of 10 Malpighian tubules was used as its own control. The concentrations of aedeskinin-III and H89 were 1 μmol l^{-1} and 20 μmol l^{-1}, respectively. Data are means ± s.e.; ***, P<0.002.

Electron microscopy

Electron micrographs of the paracellular pathway in *Aedes* Malpighian tubules reveal that septate junctions occupy most of the paracellular pathway from the apical to basal poles of epithelial

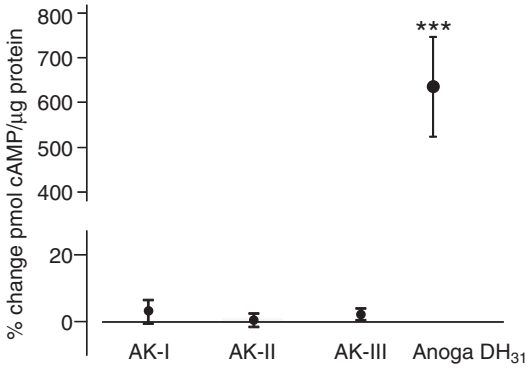

Fig. 5. The lack of effect of aedeskinins (1 μmol l^{-1}) on intracellular cAMP levels in Malpighian tubules of *Aedes aegypti*. AnogaDH_{31} (1 μmol l^{-1}) is known to increase intracellular [cAMP] in *Aedes* and *Anopheles* Malpighian tubules (Coast et al., 2005). In the present study, AnogaDH_{31} served as a positive control for the bioassay. Data are means ± s.e.; ***, P<0.001.

cells (Fig. 6A,B). Along the length of a given septate junction, the septa can occur at regular intervals, irregular intervals or there might be no septa at all (Fig. 6C). The intracellular meshwork immediately below the plasma membrane of a septate junction might present components of the cytoskeleton (Fig. 6C). Further into the cytoplasm is evidence of microtubules running perpendicular to or parallel with septate junctions (Fig. 6C). The paracellular pathway of invertebrate epithelia is thought to include a subapical region, an adherens junction and septate junctions. Distinct subapical regions and adherens junctions were not observed in the present set of electron micrographs of *Aedes* Malpighian tubules, which does not rule out their existence. In some images, the septate junction extended all the way to the brush border apical membrane (Fig. 6C).

Discussion

It is said that the study of proteomics is a 'hypothesis generator'. The present study is a case in point. Gels of cytosolic proteins of control and aedeskinin-treated tubules have identified 128 proteins and phosphoproteins that changed significantly after treating Malpighian tubules with aedeskinin-III. From these, we have selected for discussion only those proteins that might be involved in aedeskinin signaling and the consequent increase in transepithelial fluid secretion. The focus on these proteins suggests that aedeskinin-III assembles the V-type H^+ ATPase at the apical membrane and remodels the paracellular pathway.

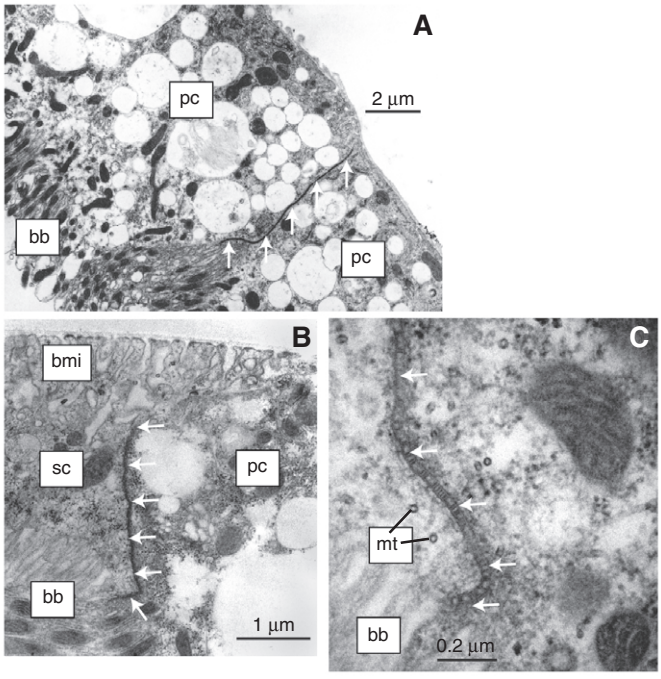

Fig. 6. The paracellular pathway in Malpighian tubules of *Aedes aegypti*. (A) The paracellular pathway between two principal cells and part of a stellate cell (near the apical brush border). Mitochondria in microvilli of the brush border are unique to principal cells of the tubule. Microvilli of the brush border of stellate cells are devoid of mitochondria. (B,C) The paracellular pathway between a stellate cell and principal cell is occupied largely by a septate junction. Septa give rise to the ladder-like structure of the junction. Note that the septate junction can extend from apical to basal poles of epithelial cells. Abbreviations: bb, brush border; bmi, basolateral membrane infoldings; mt, microtubule; pc, principal cell; sc, stellate cell. White arrows point to the paracellular pathway in B and to septa in C.

Hypothesis 1: aedeskinin-III signals to the V-type H^+ ATPase

The V-type H^+ ATPase is a proton pump that consists of two multi-subunit ring structures: a cytoplasmic V_1 complex and a membrane-embedded V_0 complex (Fig. 7A). Subunits A and B are part of the catalytic V_1 complex that mediates the hydrolysis of ATP. Subunits c are part of the V_0 complex that mediate the 'pumping' of H^+ across the membrane. Mechanically, the V-type H^+ ATPase is a motor, with V_1 and V_0 complexes operating as a stator and a rotor, respectively (Fig. 7B). The energy of ATP hydrolysis can drive transmembrane H^+-transport only when the stator and rotor are physically joined (Beltran and Nelson, 1992; Gräf et al., 1996; Zhang et al., 1992) and when the V_1 complex is anchored to the cytoskeleton to prevent its own rotation.

The reversible dissociation of V_1 and V_0 complexes is now considered a nearly universal mechanism for regulating the physiological activity of V-type H^+ ATPases (Fig. 7C). The V_1 complex can detach from the V_0 complex when H^+ transport is no longer needed. For example, when the tobacco hornworm ceases to feed or is forced to starve, the V_1 complex separates from the V_0 complex, thereby entering the cytoplasm (Sumner et al., 1995). Likewise, glucose (nutrient) deprivation causes the V_1 complex to separate from the V_0 complex in yeast (Kane, 1995). Should the need for H^+ transport arise again, the V_1 complex leaves the cytoplasm to join its partner in the membrane again.

In view of the central role of the V-type H^+ ATPase in transepithelial electrolyte and fluid secretion in Malpighian tubules of insects (Beyenbach et al., 2000), it is expected that an increase in transepithelial electrolyte and fluid secretion – stimulated by a diuretic agent such as aedeskinin – increases the transport activity of the V-type H^+ ATPase (Beyenbach, 2001). One way to increase transport activity is to increase the number of active transport pumps by joining V_1 and V_0 complexes, which removes the V_1 complex from the cytoplasm, as witnessed in the present study by subunits A and B diminishing in the cytosol after tubules have been stimulated with aedeskinin-III (Table 1).

Subunit C of the V_1 complex (not to be confused with subunit c of the V_0 complex) appears to play the pivotal role in joining the V_1 complex to the V_0 complex (Fig. 7C), as gleaned from studies of salivary glands of the blowfly. In brief, serotonin, the natural stimulant of the salivary gland, stimulates fluid secretion by means of cAMP and protein kinase A (Dames et al., 2006; Rein et al., 2008). Protein kinase A (PKA) exclusively phosphorylates subunit C as the molecular switch that joins V_1 and V_0 complexes to activate ATP hydrolysis and proton transport (Rein et al., 2008; Voss et al., 2007). Immunohistochemical studies show further that, upon serotonin stimulation, subunits C and B of the V_1 complex, PKA and actin all localize to the apical membrane of the salivary gland epithelial cell (Rein et al., 2008; Voss et al., 2007). Actin might be recruited to the apical membrane in an apparent fortification of the cytoskeleton for anchoring the V_1 complex and the holoenzyme in place (Vitavska et al., 2005; Vitavska et al., 2003; Wieczorek et al., 2003).

In the present study, the role for PKA in the kinin-stimulated diuresis is supported by (1) the decrease of subunits A and B of the V-type H^+ ATPase in the cytosol (Table 1), (2) the decrease in the regulatory subunit type II of PKA (Table 1) and (3) the reversal of the effect of aedeskinin-III on transepithelial fluid secretion by H89, an inhibitor of protein kinase A (Fig. 4). However, inconsistent with a role for PKA is the lack of effect of any aedeskinin on intracellular cAMP levels after 2 min of stimulation (Fig. 5), which confirms previous observations of cAMP-independent diuretic effects of (1) aedeskinins in *Aedes* Malpighian

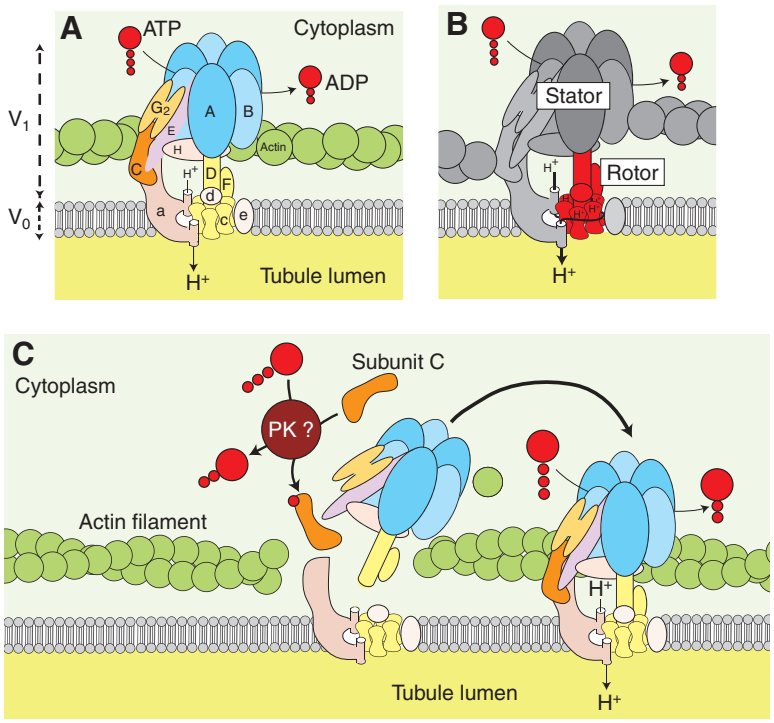

Fig. 7. Molecular, mechanical and regulatory models of the V-type H^+ ATPase. (A) Molecular model. Subunits of catalytic complex V_1 bear capital letters; subunits of the V_0 complex in the apical membrane bear small letters. (B) Mechanical model of the proton pump consisting of a stator and rotor. (C) Regulatory model. The phosphorylation of subunit C is thought to be instrumental in the assembly of the two complexes to form the active proton pump. Candidate kinases (PK) that might phosphorylate subunit C are protein kinase A and/or protein kinase C.

tubules (Cady and Hagedorn, 1999) and (2) drosokinin in *Drosophila* Malpighian tubules (Terhzaz et al., 1999).

The dilemma posed by the above conflicting observations would be solved by a stimulation of PKA that is independent of cAMP (Fig. 7C). Such a mechanism has been observed in mammalian cells. It is the NF-κB signaling pathway that targets regulated proteolysis (Zhong et al., 1997). In brief, stimulation of the NF-κB signaling pathway leads to the proteolytic degradation of IKB, an inhibitory protein of not only the transcription factor NF-κB but also of the catalytic subunit of PKA (PKA_{cat}). Thus, activation of the NF-κB signaling pathway could activate PKA_{cat}, bringing about the assembly of the V-type H^+ ATPase without an increase in intracellular cAMP (Fig. 7). Of interest is that protein kinase C (PKC) can activate the NF-κB signaling pathway (McAllister-Lucas et al., 2001; Steffan et al., 1995). The NF-κB signaling pathway occurs in insects, where one of the insect IKB proteins is known as the *Drosophila* cactus protein (Belvin et al., 1995). Alternatively, it is possible that PKC phosphorylates subunit C directly, which leaves open the question of whether PKA or PKC mediates the assembly and activation of the V-type H^+ ATPase in *Aedes* Malpighian tubules (Fig. 7C).

Hypothesis 2: aedeskinin-III signals to the paracellular pathway

The kinins are known to increase the transepithelial Cl^- conductance of Malpighian tubules as part of the diuretic mechanism for increasing the transepithelial secretion of NaCl, KCl and water (Fig. 1). Stellate cells provide the route for Cl^- secretion in *Drosophila* Malpighian tubules (O'Donnell et al., 1996; O'Donnell et al., 1998). Stellate cells might also do so in Malpighian tubules of *Aedes aegypti* under resting, control conditions (O'Connor and Beyenbach, 2001). However, upon stimulation with kinin diuretic peptides, the major route for transepithelial Cl^- secretion is between epithelial cells (Beyenbach, 2003; Pannabecker et al., 1993; Yu and Beyenbach, 2001; Yu and Beyenbach, 2004).

Ca^{2+} plays a major role in mediating the effects of kinin peptides on paracellular Cl^- conductance because the effects of kinins can be duplicated by A23187, an ionophore that allows Ca^{2+} to enter cells from the peritubular Ringer solution (Clark et al., 1998). Our proteomic study is consistent with the signaling role of Ca^{2+} because three Ca^{2+}-binding proteins are affected by aedeskinin-III: calreticulin, endoplasmin and regucalcin (Table 1).

Possessing as many as 50 Ca^{2+}-binding sites, calreticulin is a major Ca^{2+}-binding protein and therefore an important regulator of Ca^{2+} signaling (Coppolino and Dedhar, 1998; Yamaguchi, 2005), including signaling to cell-adhesion molecules (Coppolino and Dedhar, 1999; Coppolino et al., 1997). The departure of calreticulin and endoplasmin from the cytosol is expected to increase the concentration of free Ca^{2+} in the cytoplasm, thereby enhancing the effects of Ca^{2+} (Table 1). By contrast, the arrival of regucalcin in the cytosol is expected to decrease the free $[Ca^{2+}]$ in the cytoplasm through the activation of Ca^{2+}-uptake pumps in the endoplasmic/sarcoplasmic reticulum (intracellular Ca^{2+} stores) and mitochondria (Yamaguchi, 2005).

Extracellular Ca^{2+} is needed to sustain the stimulatory effects of the kinins in Malpighian tubules (Yu and Beyenbach, 2002). Detailed studies in Malpighian tubules of *Aedes aegypti* have elucidated the following signaling pathway that leads to the elevation of intracellular $[Ca^{2+}]$, as illustrated in Fig. 8. The binding of aedeskinin to its G-protein-coupled receptor activates phospholipase C, which converts phosphatidylinositol (4,5)-bisphosphate into two intracellular messengers: membrane-associated diacylglycerol (DAG) and cytoplasmic inositol (1,4,5)-trisphosphate $[Ins(1,4,5)P_3]$. The binding of $Ins(1,4,5)P_3$ to receptors at the endoplasmic reticulum opens Ca^{2+} channels, allowing the entry of Ca^{2+} into the cytoplasm. As the $[Ca^{2+}]$ in the cytoplasm rapidly rises, the rapid fall of the $[Ca^{2+}]$ in the endoplasmic reticulum triggers the opening of Ca^{2+} channels in the plasma membrane by means of a 'store-depletion mechanism'. Ca^{2+} enters the cell, raising the intracellular $[Ca^{2+}]$ even more

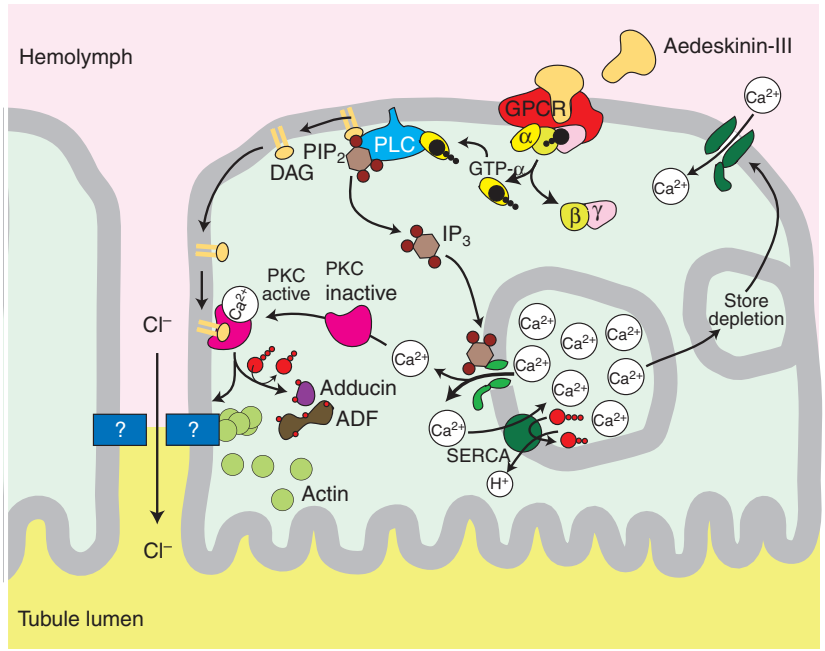

Fig. 8. Hypothetical model of aedeskinin-III signaling to the paracellular pathway in Malpighian tubules of the yellow-fever mosquito. The paracellular protein complex consists of cytoplasmic elements such as the cytoskeleton, scaffolding and regulatory proteins, and integral membrane proteins reaching into the paracellular space. The proteins defining the paracellular barrier/permeability properties are unknown in insect epithelia. ADF, actin depolymerizing factor; GPCR, G-protein-coupled receptor; α,β,γ, subunits of G protein; GTP, guanosine triphosphate; PLC, phospholipase C; PIP_2, phosphatidylinositol (4,5)-bisphosphate; DAG, diacylglycerol; PKC, protein kinase C; SERCA, sarcoplasmic and endoplasmic reticulum calcium ATPase.

(Fig. 8). Ca^{2+} binding to inactive PKC allows PKC to interact with DAG in the plasma membrane, thus targeting PKC to the membrane. When PKC binds to DAG, the kinase is activated. As the active PKC is now membrane bound, phosphorylations are limited to substrates in close proximity to the membrane and cytoskeleton (Fig. 8).

One known substrate of PKC is adducin (Matsuoka et al., 1998). Adducin is a membrane-skeletal protein found at the junctions of actin and spectrin that colocalize at sites of cell–cell contact (Kaiser et al., 1993; Kaiser et al., 1989). The phosphorylation of adducin by rho kinase promotes the association of F-actin and spectrin to form a spectrin–actin meshwork beneath the plasma membrane (Fukata et al., 1999; Gardner and Bennett, 1987; Kimura et al., 1998; Li et al., 1998). Phosphorylation by PKC inhibits the actin-capping and spectrin-recruiting activities of adducin, thereby destabilizing the cytoskeleton (Matsuoka et al., 1998). The appearance of phosphorylated adducin in the cytosol after aedeskinin treatment is consistent with the destabilization and remodeling of the cytoskeleton (Table 1; Fig. 8).

The reorganization of the cytoskeleton is further supported by the appearance in the cytosol of (1) ADF and (2) actin (Table 1; Fig. 8). If this cytoskeletal remodeling takes place along the paracellular pathway, it might mediate the switch-like increase in paracellular Cl^- conductance when kinin diuretic peptides trigger diuresis in Malpighian tubules (Fig. 8). The cytoskeletal remodeling of the paracellular pathway might include vesicular traffic to and from the paracellular pathway, as indicated by the decrease in cytoplasmic rab GDI in the presence of aedeskinin-III (Table 1). GDI mediates in part the trafficking of vesicles between donor membranes and target membranes (Stein et al., 2003). Rab is a small G protein that is found at tight junctions in polarized cells (Zahraoui et al., 1994). Accordingly, the aedeskinin-triggered diuresis might involve the trafficking of proteins between the plasma membrane and submembrane vesicles in regions of the paracellular pathway. The above discussion makes clear that the sudden increase in paracellular Cl^- conductance triggered by kinin diuretic peptides requires the paracellular pathway functioning as a continuum between extracellular and intracellular components.

The paracellular pathway in Malpighian tubules of *Aedes aegypti*

Studies of vertebrate epithelia have taken the lead in our understanding of the physiological regulation of the paracellular transport pathway (Anderson and Van Itallie, 1995; Cereijido, 1991; Hopkins et al., 2000; Madara, 1998). In particular, the regulation of the paracellular pathway has been localized to the tight junction (Hopkins et al., 2003; Kahle et al., 2004; Schneeberger and Lynch, 2004; Shen et al., 2008). The regulation of the paracellular pathway in invertebrates has been researched far less, even though Malpighian tubules display the most dynamic and dramatic changes in a paracellular transport activity (Beyenbach, 2003; Pannabecker et al., 1993; Yu and Beyenbach, 2002; Yu and Beyenbach, 2004). It raises questions about the differences between tight and septate junctions that enable septate junctions to respond to signaling with switch-like speed and with a wide dynamic range of paracellular electrical conductance.

In electron micrographs, tight junctions in vertebrates and septate junctions in invertebrates have very different geometries. Tight junctions are located at the most apical region of epithelial cells, and they extend into the paracellular pathway for only a short distance, less than 1 μm. Moreover, tight junctions are points of contact between neighboring cells that are formed by the interaction of the extracellular loops of the integral membrane proteins claudin and occludin (Furuse et al., 1998; Ikenouchi et al., 2005). Interactions of these extracellular loops obliterate the extracellular space and give the appearance of the focal fusion of the plasma membranes of neighboring cells. Beyond the less than 1 μm region of the vertebrate tight junction, the lateral interstitial space accounts for more than 95% of the length of the paracellular pathway, given a conservative epithelial cell height of 20 μm.

In marked contrast, septate junctions span the whole height of the epithelial cell from apical to basal poles of epithelial cells over the length of many microns (Fig. 6). Ladder-like septa appear to make sure that the lateral plasma membranes of adjacent cells do not fuse. They are kept approximately 160 Å apart (Fig. 6C). What forms the rungs of the paracellular ladder is unknown. The

constitution of the electron-dense material in the space between septa is also unknown.

In view of the wide paracellular space (160 Å) and the small molecular diameters of Na^+, K^+, Cl^- and water (<5 Å), it follows that the usual solutes of hemolymph (including glucose, 70 Å) can occupy the intercellular septate junctional space – unless septa prevent access. Preventing access might account for the barrier function of septate junctions. By contrast, a reversible, zipper-like opening of septa would provide access, thereby increasing the paracellular conductance/permeability. Such an increase would be expected to be substantial in view of the width –160 Å – of the paracellular path now open.

In vertebrate tight junctions, claudins and occludins provide the barrier and permselectivity properties of the tight junction. Moreover, claudins display a stunning spontaneous breaking and resealing (Sasaki et al., 2003). Using GFP-tagged claudin in living cells it was possible to observe claudin strands breaking, migrating and reconnecting in minutes, demonstrating what physiologically could be open and closed routes for paracellular transport. Similarly, the opening and closing of septa-forming proteins could regulate the permeability and conductance of septate junctions. The finding of claudin-like proteins, such as sinuous and megatrachea in septate junctions (Behr et al., 2003; Wu et al., 2004), raises the intriguing question of whether septate junctions also undergo spontaneous turnover and remodeling.

What the present proteomic study urges is therefore the identification of (1) the proteins that form the ladder of septate junctions and (2) their scaffolding proteins on the cytoplasmic side. These interactions might mediate the switch-like on/off changes in paracellular Cl^- conductance that meet the diuretic and antidiuretic needs of the insect.

This work was supported by grants from the NIH (R21 AI072102) and the National Science Foundation (IOB-0542797). The authors acknowledge the capable technical contributions of Robert W. Sherwood in the Proteomics and Mass Spectrometry Core Facility of Cornell University. We are also indebted to Stephen Schepel, Austin Blum, Tiffany Sou, Mohammed Khattab and Andrew Fox, who helped collect Malpighian tubules for proteomic analysis. Deposited in PMC for release after 12 months.

References

Anderson, J. M. and Van Itallie, C. M. (1995). Tight junctions and the molecular basis for regulation of paracellular permeability. *Am. J. Physiol.* **269**, G467-G475.

Behr, M., Riedel, D. and Schuh, R. (2003). The claudin-like megatrachea is essential in septate junctions for the epithelial barrier function in *Drosophila*. *Dev. Cell* **5**, 611-620.

Beltran, C. and Nelson, N. (1992). The membrane sector of vauolar H^+-ATPase by itself is impermeable to protons. *Acta Physiol. Scand.* **Suppl. 607**, 41-47.

Belvin, M. P., Jin, Y. and Anderson, K. V. (1995). Cactus protein degradation mediates *Drosophila* dorsal-ventral signaling. *Genes Dev.* **9**, 783-793.

Beyenbach, K. W. (2001). Energizing epithelial transport with the vacuolar H^+-ATPase. *News Physiol. Sci.* **16**, 145-151.

Beyenbach, K. W. (2003). Regulation of tight junction permeability with switch-like speed. *Curr. Opin. Nephrol. Hypertens.* **12**, 543-550.

Beyenbach, K. W., Pannabecker, T. L. and Nagel, W. (2000). Central role of the apical membrane H^+-ATPase in electrogenesis and epithelial transport in Malpighian tubules. *J. Exp. Biol.* **203**, 1459-1468.

Cady, C. and Hagedorn, H. H. (1999). Effects of putative diuretic factors on intracellular secondary messenger levels in the Malpighian tubules of *Aedes aegypti*. *J. Insect Physiol.* **45**, 327-337.

Cereijido, M. (1991). *Tight Junctions.* Boca Raton, FL: CRC Press.

Clark, T. M., Hayes, T. K., Holman, G. M. and Beyenbach, K. W. (1998). The concentration-dependence of CRF-like diuretic peptide: mechanisms of action. *J. Exp. Biol.* **201**, 1753-1762.

Coast, G. M. (1995). Synergism between diuretic peptides controlling ion and fluid transport in insect malpighian tubules. *Regul. Pept.* **57**, 283-296.

Coast, G. M., Garside, C. S., Webster, S. G., Schegg, K. M. and Schooley, D. A. (2005). Mosquito natriuretic peptide identified as a calcitonin-like diuretic hormone in *Anopheles gambiae* (Giles). *J. Exp. Biol.* **208**, 3281-3291.

Coppolino, M. G. and Dedhar, S. (1998). Calreticulin. *Int. J. Biochem. Cell Biol.* **30**, 553-558.

Coppolino, M. G. and Dedhar, S. (1999). Ligand-specific, transient interaction between integrins and calreticulin during cell adhesion to extracellular matrix proteins is dependent upon phosphorylation/dephosphorylation events. *Biochem. J.* **340**, 41-50.

Coppolino, M. G., Woodside, M. J., Demaurex, N., Grinstein, S., St-Arnaud, R. and Dedhar, S. (1997). Calreticulin is essential for integrin-mediated calcium signalling and cell adhesion. *Nature* **386**, 843-847.

Dames, P., Zimmermann, B., Schmidt, R., Rein, J., Voss, M., Schewe, B., Walz, B. and Baumann, O. (2006). cAMP regulates plasma membrane vacuolar-type H^+-ATPase assembly and activity in blowfly salivary glands. *Proc. Natl. Acad. Sci. USA* **103**, 3926-3931.

Davies, S. P., Reddy, H., Caivano, M. and Cohen, P. (2000). Specificity and mechanism of action of some commonly used protein kinase inhibitors. *Biochem. J.* **351**, 95-105.

Fukata, Y., Oshiro, N., Kinoshita, N., Kawano, Y., Matsuoka, Y., Bennett, V., Matsuura, Y. and Kaibuchi, K. (1999). Phosphorylation of adducin by Rho-kinase plays a crucial role in cell motility. *J. Cell Biol.* **145**, 347-361.

Furuse, M., Fujita, K., Hiiragi, T., Fujimoto, K. and Tsukita, S. (1998). Claudin-1 and -2: novel integral membrane proteins localizing at tight junctions with no sequence similarity to occludin. *J. Cell Biol.* **141**, 1539-1550.

Gardner, K. and Bennett, V. (1987). Modulation of spectrin-actin assembly by erythrocyte adducin. *Nature* **328**, 359-362.

Gräf, R., Harvey, W. R. and Wieczorek, H. (1996). Purification and properties of a cytosolic V_1-ATPase. *J. Biol. Chem.* **271**, 20908-20913.

Hayes, T. K., Pannabecker, T. L., Hinckley, D. J., Holman, G. M., Nachman, R. J., Petzel, D. H. and Beyenbach, K. W. (1989). Leucokinins, a new family of ion transport stimulators and inhibitors in insect Malpighian tubules. *Life Sci.* **44**, 1259-1266.

Holman, G. M., Cook, B. J. and Nachman, R. J. (1987). Isolation, primary structure and synthesis of leucokinin-VII and VIII: the final members of the new family of cephalomyotropic peptides isolated from head extracts of *Leucophaea maderae*. *Comp. Biochem. Physiol.* **88**, 31-34.

Hopkins, A. M., Li, D., Mrsny, R. J., Walsh, S. V. and Nusrat, A. (2000). Modulation of tight junction function by G protein-coupled events. *Adv. Drug Deliv. Rev.* **41**, 329-340.

Hopkins, A. M., Walsh, S. V., Verkade, P., Boquet, P. and Nusrat, A. (2003). Constitutive activation of Rho proteins by CNF-1 influences tight junction structure and epithelial barrier function. *J. Cell Sci.* **116**, 725-742.

Ikenouchi, J., Furuse, M., Furuse, K., Sasaki, H. and Tsukita, S. (2005). Tricellulin constitutes a novel barrier at tricellular contacts of epithelial cells. *J. Cell Biol.* **171**, 939-945.

Kahle, K. T., Wilson, F. H., Lalioti, M., Toka, H., Qin, H. and Lifton, R. P. (2004). WNK kinases: molecular regulators of integrated epithelial ion transport. *Curr. Opin. Nephrol. Hypertens.* **13**, 557-562.

Kaiser, H. W., O'Keefe, E. and Bennett, V. (1989). Adducin: Ca^{++}-dependent association with sites of cell-cell contact. *J. Cell Biol.* **109**, 557-569.

Kaiser, H. W., Ness, W., O'Keefe, E., Balcerkiewicz, A. and Kreysel, H. W. (1993). Localization of adducin in epidermis. *J. Invest. Dermatol.* **101**, 783-788.

Kane, P. M. (1995). Disassembly and reassembly of the yeast vacuolar H^+-ATPase *in vivo*. *J. Biol. Chem.* **270**, 17025-17032.

Kimura, K., Fukata, Y., Matsuoka, Y., Bennett, V., Matsuura, Y., Okawa, K., Iwamatsu, A. and Kaibuchi, K. (1998). Regulation of the association of adducin with actin filaments by Rho-associated kinase (Rho-kinase) and myosin phosphatase. *J. Biol. Chem.* **273**, 5542-5548.

Li, X., Matsuoka, Y. and Bennett, V. (1998). Adducin preferentially recruits spectrin to the fast growing ends of actin filaments in a complex requiring the MARCKS-related domain and a newly defined oligomerization domain. *J. Biol. Chem.* **273**, 19329-19338.

Madara, J. L. (1998). Regulation of the movement of solutes across tight junctions. *Annu. Rev. Physiol.* **60**, 143-159.

Matsuoka, Y., Li, X. and Bennett, V. (1998). Adducin is an *in vivo* substrate for protein kinase C: phosphorylation in the MARCKS-related domain inhibits activity in promoting spectrin-actin complexes and occurs in many cells, including dendritic spines of neurons. *J. Cell Biol.* **142**, 485-497.

McAllister-Lucas, L. M., Inohara, N., Lucas, P. C., Ruland, J., Benito, A., Li, Q., Chen, S., Chen, F. F., Yamaoka, S., Verma, I. M. et al. (2001). Bimp1, a MAGUK family member linking protein kinase C activation to Bcl10-mediated NF-kappaB induction. *J. Biol. Chem.* **276**, 30589-30597.

O'Connor, K. R. and Beyenbach, K. W. (2001). Chloride channels in apical membrane patches of stellate cells of Malpighian tubules of *Aedes aegypti*. *J. Exp. Biol.* **204**, 367-378.

O'Donnell, M. J. and Spring, J. H. (2000). Modes of control of insect Malpighian tubules: Synergism, antagonism, cooperation and autonomous regulation. *J. Insect Physiol.* **46**, 107-117.

O'Donnell, M. J., Dow, J. A., Huesmann, G. R., Tublitz, N. J. and Maddrell, S. H. (1996). Separate control of anion and cation transport in Malpighian tubules of *Drosophila melanogaster*. *J. Exp. Biol.* **199**, 1163-1175.

O'Donnell, M. J., Rheault, M. R., Davies, S. A., Rosay, P., Harvey, B. J., Maddrell, S. H., Kaiser, K. and Dow, J. A. (1998). Hormonally controlled chloride movement across *Drosophila* tubules is via ion channels in stellate cells. *Am. J. Physiol.* **274**, R1039-R1049.

Pannabecker, T. L., Hayes, T. K. and Beyenbach, K. W. (1993). Regulation of epithelial shunt conductance by the peptide leucokinin. *J. Membr. Biol.* **132**, 63-76.

Ramsay, J. A. (1953). Active transport of potassium by the Malpighian tubules of insects. *J. Exp. Biol.* **93**, 358-369.

Rein, J., Voss Blenau, W., Walz, B. and Baumann, O. (2008). Hormone-induced assembly and activation of V-ATPase in blowfly salivary glands is mediated by protein kinase A. *Am. J. Physiol. Cell Physiol.* **294**, C56-C65.

Rescher, U., Ludwig, C., Konietzko, V., Kharitonenkov, A. and Gerke, V. (2008). Tyrosine phosphorylation of annexin A2 regulates Rho-mediated actin rearrangement and cell adhesion. *J. Cell Sci.* **121**, 2177-2185.

Sasaki, H., Matsui, C., Furuse, K., Mimori-Kiyosue, Y., Furuse, M. and Tsukita, S. (2003). Dynamic behavior of paired claudin strands within apposing plasma membranes. *Proc. Natl. Acad. Sci. USA* **100**, 3971-3976.
Schneeberger, E. E. and Lynch, R. D. (2004). The tight junction: a multifunctional complex. *Am. J. Physiol. Cell Physiol.* **286**, C1213-C1228.
Shen, L., Weber, C. R. and Turner, J. R. (2008). The tight junction protein complex undergoes rapid and continuous molecular remodeling at steady state. *J. Cell Biol.* **181**, 683-695.
Shevchenko, A., Wilm, M., Vorm, O. and Mann, M. (1996). Mass spectrometric sequencing of proteins silver-stained polyacrylamide gels. *Anal. Chem.* **68**, 850-858.
Steffan, N. M., Bren, G. D., Frantz, B., Tocci, M. J., O'Neill, E. A. and Paya, C. V. (1995). Regulation of IkB alpha phosphorylation by PKC- and Ca(2+)-dependent signal transduction pathways. *J. Immunol.* **155**, 4685-4691.
Stein, M. P., Dong, J. and Wandinger-Ness, A. (2003). Rab proteins and endocytic trafficking: potential targets for therapeutic intervention. *Adv. Drug Deliv. Rev.* **55**, 1421-1437.
Sumner, J. P., Dow, J. A., Earley, F. G., Klein, U., Jäger, D. and Wieczorek, H. (1995). Regulation of plasma membrane V-ATPase activity by dissociation of peripheral subunits. *J. Biol. Chem.* **270**, 5649-5653.
Terhzaz, S., O'Connell, F. C., Pollock, V. P., Kean, L., Davies, S. A., Veenstra, J. A. and Dow, J. A. T. (1999). Isolation and characterization of a leucokinin-like peptide of *Drosophila melanogaster*. *J. Exp. Biol.* **202**, 3667-3676.
Torfs, P., Nieto, J., Veelaert, D., Boon, D., van de Water, G., Waelkens, E., Derua, R., Calderon, J., de Loof, A. and Schoofs, L. (1999). The kinin peptide family in invertebrates. *Ann. NY Acad. Sci.* **897**, 361-373.
Veenstra, J. A., Pattillo, J. M. and Petzel, D. H. (1997). A single cDNA encodes all three *Aedes* leucokinins, which stimulate both fluid secretion by the Malpighian tubules and hindgut contractions. *J. Biol. Chem.* **272**, 10402-10407.
Vitavska, O., Wieczorek, H. and Merzendorfer, H. (2003). A novel role for subunit C in mediating binding of the H^+-V-ATPase to the actin cytoskeleton. *J. Biol. Chem.* **278**, 18499-18505.
Vitavska, O., Merzendorfer, H. and Wieczorek, H. (2005). The V-ATPase subunit C binds to polymeric F-actin as well as monomeric G-actin and induces cross-linking of actin filaments. *J. Biol. Chem.* **280**, 1070-1076.
Voss, M., Vitavska, O., Walz, B., Wieczorek, H. and Baumann, O. (2007). Stimulus-induced phosphorylation of vacuolar H^+-ATPase by protein kinase A. *J. Biol. Chem.* **282**, 33735-33742.
Wieczorek, H., Huss, M., Merzendorfer, H., Reineke, S., Vitavska, O. and Zeiske, W. (2003). The insect plasma membrane H^+ V-ATPase: intra-, inter-, and supramolecular aspects. *J. Bioenerg. Biomembr.* **35**, 359-366.
Wu, V. M., Schulte, J., Hirschi, A., Tepass, U. and Beitel, G. J. (2004). Sinuous is a *Drosophila* claudin required for septate junction organization and epithelial tube size control. *J. Cell Biol.* **164**, 313-323.
Yamaguchi, M. (2005). Role of regucalcin in maintaining cell homeostasis and function (review). *Int. J. Mol. Med.* **15**, 371-389.
Yang, Y., Thannhauser, T. W., Li, L. and Zhang, S. (2007). Development of an integrated approach for evaluation of 2-D gel image analysis: impact of multiple proteins in single spots on comparative proteomics in conventional 2-D gel/MALDI workflow. *Electrophoresis* **28**, 2080-2094.
Yu, M. and Beyenbach, K. W. (2001). Leucokinin and the modulation of the shunt pathway in Malpighian tubules. *J. Insect Physiol.* **47**, 263-276.
Yu, M. J. and Beyenbach, K. W. (2002). Leucokinin activates Ca^{2+}-dependent signal pathway in principal cells of *Aedes aegypti* Malpighian tubules. *Am. J. Physiol.* **283**, F499-F508.
Yu, M. J. and Beyenbach, K. W. (2004). Effects of leucokinin-VIII on *Aedes* Malpighian tubule segments lacking stellate cells. *J. Exp. Biol.* **207**, 519-526.
Zahraoui, A., Joberty, G., Arpin, M., Fontaine, J. J., Hellio, R., Tavitian, A. and Louvard, D. (1994). A small rab GTPase is distributed in cytoplasmic vesicles in non polarized cells but colocalizes with the tight junction marker ZO-1 in polarized epithelial cells. *J. Cell Biol.* **124**, 101-115.
Zhang, J., Myers, M. and Forgac, M. (1992). Characterization of the V_0 domain of the coated vesicle H^+-ATPase. *J. Biol. Chem.* **267**, 9773-9778.
Zhong, H., SuYang, H., Erdjument-Bromage, H., Tempst, P. and Ghosh, S. (1997). The transcriptional activity of NF-kappaB is regulated by the IkappaB-associated PKAc subunit through a cyclic AMP-independent mechanism. *Cell* **89**, 413-424.
Zubrzak, P., Williams, H., Coast, G. M., Isaac, R. E., Reyes-Rangel, G., Juaristi, E., Zabrocki, J. and Nachman, R. J. (2007). Beta-amino acid analogs of an insect neuropeptide feature potent bioactivity and resistance to peptidase hydrolysis. *Biopolymers* **88**, 76-82.